

Shedding Light on the “Dark Side” of $B_d^0-\overline{B}_d^0$ Mixing through $B_d \rightarrow \pi^+\pi^-$, $K \rightarrow \pi\nu\bar{\nu}$ and $B_{d,s} \rightarrow \mu^+\mu^-$

Robert Fleischer,^a Gino Isidori,^b Joaquim Matias^c

^a *Theory Division, CERN, CH-1211 Geneva 23, Switzerland*

^b *INFN, Laboratori Nazionali di Frascati, I-00044 Frascati, Italy*

^c *IFAE, Universitat Autònoma de Barcelona, 08193 Bellaterra, Barcelona, Spain*

Abstract

In a wide class of new-physics models, which can be motivated through generic arguments and within supersymmetry, we obtain large contributions to $B_d^0-\overline{B}_d^0$ mixing, but not to $\Delta B = 1$ processes. If we assume such a scenario, the solutions $\phi_d \sim 47^\circ \vee 133^\circ$ for the $B_d^0-\overline{B}_d^0$ mixing phase implied by $\mathcal{A}_{\text{CP}}^{\text{mix}}(B_d \rightarrow J/\psi K_S)$ cannot be converted directly into a constraint in the $\overline{\rho}-\overline{\eta}$ plane. However, we may complement ϕ_d with $|V_{ub}/V_{cb}|$ and the recently measured CP asymmetries in $B_d \rightarrow \pi^+\pi^-$ to determine the unitarity triangle, with its angles α , β and γ . To this end, we have also to control penguin effects, which we do by means of the CP-averaged $B_d \rightarrow \pi^\mp K^\pm$ branching ratio. Interestingly, the present data show a perfectly consistent picture not only for the “standard” solution of $\phi_d \sim 47^\circ$, but also for $\phi_d \sim 133^\circ$. In the latter case, the preferred region for the apex of the unitarity triangle is in the second quadrant, allowing us to accommodate conveniently $\gamma > 90^\circ$, which is also favoured by other non-leptonic B decays such as $B \rightarrow \pi K$. Moreover, also the prediction for $\text{BR}(K^+ \rightarrow \pi^+\nu\bar{\nu})$ can be brought to better agreement with experiment. Further strategies to explore this scenario with the help of $B_{d,s} \rightarrow \mu^+\mu^-$ decays are discussed as well.

1 Introduction

Thanks to the efforts at the B factories, the exploration of CP violation is now entering another exciting stage, allowing us to confront the Kobayashi–Maskawa mechanism [1] with data. After the discovery of mixing-induced CP violation in the “gold-plated” mode $B_d \rightarrow J/\psi K_S$ [2], as well as important other measurements, one of the most interesting questions is now to what extent the possible space for new physics (NP) has already been reduced. In this context, the central target is the unitarity triangle of the Cabibbo–Kobayashi–Maskawa (CKM) matrix illustrated in Fig. 1(a), where $\bar{\rho}$ and $\bar{\eta}$ are the generalized Wolfenstein parameters [3]. The usual fits for the allowed region for the apex of the unitarity triangle in the $\bar{\rho}$ – $\bar{\eta}$ plane – the “CKM fits” – seem to indicate that no NP is required to accommodate the data [4, 5]. However, this is not the complete answer to this exciting question. In order to fully address it, the interpretation of the data on the mixing-induced CP asymmetry¹

$$\mathcal{A}_{\text{CP}}^{\text{mix}}(B_d \rightarrow J/\psi K_S) = -\sin \phi_d, \quad (1)$$

where ϕ_d is the CP-violating weak B_d^0 – \overline{B}_d^0 mixing phase, requires a more involved analysis. Within the Standard Model (SM), ϕ_d is given by 2β . However, due to the possible impact of physics beyond the SM, ϕ_d takes the following general form:

$$\phi_d = \phi_d^{\text{SM}} + \phi_d^{\text{NP}} = 2\beta + \phi_d^{\text{NP}}, \quad (2)$$

where ϕ_d^{NP} is due to non-standard contributions to B_d^0 – \overline{B}_d^0 mixing, which is the preferred mechanism for NP to manifest itself in (1). In principle, physics beyond the SM may also affect the $B \rightarrow J/\psi K$ decay amplitudes; however, in this case the new contributions have to compete with SM tree-level amplitudes and their relative impact is expected to be much smaller. So far, a set of “smoking-gun” observables to search for such kind of NP does not indicate any deviation from the SM [7].

Obviously, because of the ϕ_d^{NP} term in (2), we may not convert the experimental information on ϕ_d into a constraint on β in the presence of NP contributions to $B_{d,s}^0$ – $\overline{B}_{d,s}^0$ mixing. Moreover, we may not use the SM interpretation of the $B_{d,s}$ mass differences $\Delta M_{d,s}$ to determine the unitarity-triangle side

$$R_t \equiv \left| \frac{V_{td}V_{tb}^*}{V_{cd}V_{cb}^*} \right| = \frac{1}{\lambda} \left| \frac{V_{td}}{V_{cb}} \right| = \sqrt{(1 - \bar{\rho})^2 + \bar{\eta}^2}, \quad (3)$$

as recently discussed in [6, 8, 9]. On the contrary, the determination of the side

$$R_b \equiv \left| \frac{V_{ud}V_{ub}^*}{V_{cd}V_{cb}^*} \right| = \left(1 - \frac{\lambda^2}{2} \right) \frac{1}{\lambda} \left| \frac{V_{ub}}{V_{cb}} \right| = \sqrt{\bar{\rho}^2 + \bar{\eta}^2} \quad (4)$$

by means of exclusive and inclusive transitions of the type $b \rightarrow u\ell\bar{\nu}_\ell$ and $b \rightarrow c\ell\bar{\nu}_\ell$, which are dominated by SM tree-level amplitudes, is very robust as far as the impact of NP is concerned.

¹For a detailed discussion, see [6].

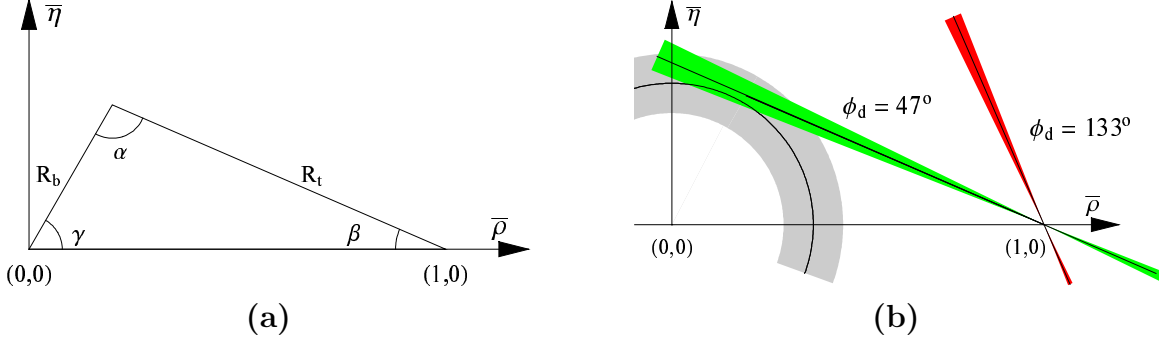


Figure 1: (a) Definition of the CKM unitarity triangle. (b) Standard procedure adopted in the literature to represent the two solutions for ϕ_d in (5); as emphasized in Section 2, this procedure is *not* correct in the case of the second “unconventional” $\phi_d = 133^\circ$ branch.

A determination of the “true” unitarity triangle in the presence of a completely general NP model, i.e. with arbitrary flavour-mixing terms, is almost impossible. However, we may still perform useful predictive analyses within certain scenarios for physics beyond the SM, for example within models with “minimal flavour violation” (MFV), where the only source for flavour mixing is still given by the CKM matrix (see, for instance, [10, 11]). In the present paper we go one step beyond the MFV models: we analyse a scenario with large generic NP contributions to $B_d^0-\overline{B}_d^0$ mixing ($\Delta B = 2$), eventually also to ε_K ($\Delta S = 2$), but *not* to the $\Delta B = 1$ and $\Delta S = 1$ decay amplitudes. As we shall demonstrate, this scenario is well motivated by simple dimensional arguments in a wide class of models, including supersymmetric frameworks.

If we assume NP of this kind, we may complement the experimental information on ϕ_d with data on CP violation in $B_d \rightarrow \pi^+\pi^-$ to extract γ , and may then fix the “true” apex of the unitarity triangle with the help of the side R_b . Needless to note, we may then also extract α and β . Since we have already strong experimental and theoretical indications for large penguin effects in $B_d \rightarrow \pi^+\pi^-$, we must definitely care about them. To this end, we follow [12, 13], and use data on the CP-averaged $B_d \rightarrow \pi^\mp K^\pm$ branching ratio, which allows us to control the penguin contributions with the help of plausible dynamical assumptions and U -spin flavour-symmetry arguments. For alternative strategies to extract physics information from ϕ_d , R_b , and CP violation in $B_d \rightarrow \pi^+\pi^-$, see, for instance, [14].

Another important aspect of our analysis are the very rare decays $K \rightarrow \pi\nu\bar{\nu}$ and $B_{d,s} \rightarrow \mu^+\mu^-$. Using the allowed ranges for the generalized Wolfenstein parameters obtained from the strategy sketched above, we are able to predict the branching ratios for these modes independently of possible NP contributions to $B_d^0-\overline{B}_d^0$ mixing. As we shall show, these predictions could be very different from the SM expectations.

The outline of this paper is as follows: a closer look at ϕ_d , R_b and β is presented in Section 2. In Section 3, we motivate the scenario where NP manifests itself only through contributions to $B_d^0-\overline{B}_d^0$ mixing. In Section 4, we discuss how we may determine the “true” unitarity triangle for this kind of NP with the help of CP violation in $B_d \rightarrow \pi^+\pi^-$. The implications for the rare decays $K \rightarrow \pi\nu\bar{\nu}$ and $B_{d,s} \rightarrow \mu^+\mu^-$ are presented in Section 5. Finally, we conclude in Section 6 with a short summary of our results and a brief outlook.

2 A Closer Look at ϕ_d , R_b and β

The present world average for $\sin \phi_d$, determined from mixing-induced CP violation in $B_d \rightarrow J/\psi K_S$ and similar modes, is $\sin \phi_d = 0.734 \pm 0.054$ [5], which implies

$$\phi_d = (47_{-4}^{+5})^\circ \vee (133_{-5}^{+4})^\circ. \quad (5)$$

Here the former solution would be in perfect agreement with the “indirect” range implied by the CKM fits, $40^\circ \lesssim \phi_d \lesssim 60^\circ$ [4], whereas the latter would show a significant discrepancy. Measuring the sign of $\cos \phi_d$, both solutions can be distinguished. There are several strategies on the market to accomplish this important task [15]. For example, in the $B \rightarrow J/\psi K$ system, $\text{sgn}(\cos \phi_d)$ can be extracted from the time-dependent angular distribution of the decay products of $B_d \rightarrow J/\psi[\rightarrow \ell^+ \ell^-] K^*[\rightarrow \pi^0 K_S]$, if the sign of a hadronic parameter $\cos \delta_f$, involving a strong phase δ_f , is fixed through factorization [16]. This analysis is already in progress at the B factories [17].

In this context, it is important to note that the CKM factor R_b introduced in (4) allows us to obtain the following bounds (see Fig. 1a):

$$(\sin \beta)_{\max} = R_b^{\max}, \quad (\sin 2\beta)_{\max} = 2R_b^{\max} \sqrt{1 - (R_b^{\max})^2}. \quad (6)$$

Using the rather conservative experimental range

$$R_b = 0.38 \pm 0.08, \quad (7)$$

which corresponds to $R_b^{\max} = 0.46$, we obtain

$$|\beta|_{\max} = 27.4^\circ. \quad (8)$$

Since the determination of R_b from semileptonic B decays, which originate from tree-level SM processes, appears to be very robust as far as the impact of NP is concerned, we may consider (8) as an upper bound for the “true” angle β of the unitarity triangle. Consequently, as we have $\phi_d = 2\beta$ within the SM, (8) implies

$$|\phi_d^{\text{SM}}|_{\max} = 2|\beta|_{\max} = 55^\circ. \quad (9)$$

Whereas the former solution $\phi_d \sim 47^\circ$ in (5) satisfies this bound nicely, this is definitely not the case for $\phi_d \sim 133^\circ$. The latter solution cannot be accommodated in the SM and requires NP contributions to $B_d^0 - \overline{B}_d^0$ mixing, i.e. we now need $\phi_d^{\text{NP}} \neq 0$ in (2). At this point, the important question of how we may represent this second solution in the $\overline{\rho} - \overline{\eta}$ plane arises. In the literature, this is usually simply done through a second branch, corresponding to

$$\beta \sim 133^\circ/2 = 66.5^\circ \quad \text{and} \quad \beta \sim -(180^\circ - 66.5^\circ) = -113.5^\circ, \quad (10)$$

as we have shown in Fig. 1(b). However, because of (2), this is actually *not* correct. Moreover, since $\phi_d \sim 133^\circ$ is associated with NP contributions to $B_d^0 - \overline{B}_d^0$ mixing, we may *no longer* use the SM interpretation of ΔM_d and $\Delta M_s/\Delta M_d$ to determine the side R_i of the unitarity triangle. In particular, we may no longer conclude from the

experimental lower bound on ΔM_s that $|\gamma| < 90^\circ$. It is important to note that (2) applies to $\phi_d \sim 47^\circ$ as well, so that NP may – at least in principle – hide itself in this case, despite the striking consistency with the SM interpretation of other observables.

As already pointed out, one of the key ingredients to determine the “true” apex of the unitarity triangle without using information on $B_d^0-\overline{B}_d^0$ mixing is the side R_b . If we complement it with a measurement of γ , we may determine the coordinates of the apex of the unitarity triangle straightforwardly through

$$\overline{\rho} = R_b \cos \gamma, \quad \overline{\eta} = R_b \sin \gamma. \quad (11)$$

From a theoretical point of view, certain pure “tree” decays would be best suited for the determination of γ , allowing theoretically clean extractions of this angle that would also be very robust under the impact of NP (see, for instance, [18]).² A similar comment applies to the new strategies that were recently proposed in [20, 21]. Here decays of the kind $B_d \rightarrow DK_{S(L)}$ and $B_s \rightarrow D\eta^{(\prime)}, D\phi, \dots$ are employed. If we use the $B_q^0-\overline{B}_q^0$ mixing phase ϕ_q as an input, and observe the neutral D mesons through their decays into CP-even and CP-odd eigenstates, certain “untagged” and mixing-induced observables allow a very efficient, theoretically clean determination of γ in an essentially unambiguous manner [20]; alternatively, we may also employ decays of the neutral D mesons into CP non-eigenstates to this end [21]. These strategies appear to be particularly interesting for the next generation of dedicated B experiments, LHCb and BTeV, as well as those at super- B factories, although important steps may already be made at BaBar and Belle.

Since we cannot yet confront these methods with data, we have to employ alternative strategies to extract γ . In this context, $B_d \rightarrow \pi^+\pi^-$ offers a very interesting tool. If we use ϕ_d as an input, and employ the CP-averaged $B_d \rightarrow \pi^\mp K^\pm$ branching ratio to control the penguin effects [12], we may determine γ from the CP-violating $B_d \rightarrow \pi^+\pi^-$ observables for each of the two solutions given in (5) [13]. In the future, the $B_d \rightarrow \pi^+\pi^-$ observables can be fully exploited with the help of $B_s \rightarrow K^+K^-$ [22]. In contrast to the pure tree decays mentioned above, these modes may in principle well be affected by new physics, as they receive contributions from loop-induced flavour-changing neutral-current (FCNC) amplitudes. However, as we shall discuss in the next section, there is a particularly interesting class of extensions of the SM where new physics yields sizeable contributions to $B_d^0-\overline{B}_d^0$ mixing only, leaving the decay amplitudes – including the loop-induced ones – almost unaffected.

3 New Physics in $B_d^0-\overline{B}_d^0$ Mixing

3.1 General Considerations

As far as flavour physics is concerned, extensions of the SM can be classified into two wide categories: models with minimal flavour violation and models with new sources of flavour mixing. Within the highly-constrained class of MFV models, the only source of flavour-symmetry breaking terms is given by the SM Yukawa couplings [11]. As a

²In principle, NP could enter in these strategies through $D^0-\overline{D}^0$ mixing. However, it could then be taken into account through a measurement of the corresponding mixing parameters [19].

consequence, all flavour-changing transitions are still ruled by the CKM matrix. For this reason, many of the standard CKM constraints hold also in MFV models: the determination of R_t in terms of $\Delta M_s/\Delta M_d$ is still valid [10], and the relation between $\sin \phi_d$ and $\sin 2\beta$ can differ at most by an overall sign [23], i.e. $\phi_d^{\text{NP}} = 0^\circ$ or $\phi_d^{\text{NP}} = 180^\circ$. It is then easy to realize that within MFV models the structure of the unitarity triangle is fixed – up to a twofold ambiguity – even without $B_d \rightarrow \pi^+\pi^-$ data, and that there is no room for the non-standard solution $\phi_d \sim 133^\circ$.

In the wide class of models with new sources of flavour mixing, it is rather natural to expect extra $\mathcal{O}(1)$ contributions to the $B_d^0\text{--}\overline{B}_d^0$ amplitude, with arbitrary phases, so that we may accommodate any value of ϕ_d^{NP} . It is also very natural to assume that these NP effects have a negligible impact on $\Delta B = 1$ amplitudes dominated by tree-level SM contributions; this happens essentially in all realistic models. On the other hand, it is less obvious why these new sources of flavour-symmetry breaking – being able to induce $\mathcal{O}(1)$ corrections to $B_d^0\text{--}\overline{B}_d^0$ mixing – should have a small impact on $\Delta B = 1$ amplitudes arising only at the loop level within the SM. This hypothesis, which is one of the main assumptions of the present analysis, certainly does not represent the most general NP scenario. However, as we shall discuss in the following, it can be realized under rather general conditions.

The generic NP scenario we shall advocate is a model where non-standard effects are negligible in all amplitudes that receive tree-level SM contributions (independently of possible CKM suppressions). Moreover, in order to protect the effects on $\Delta B = 1$ FCNC amplitudes, we shall add the following two general requirements:

- i) the effective scale of NP is substantially higher than the electroweak scale;
- ii) the adimensional effective couplings ruling $\Delta B = 2$ transitions can always be expressed as the square of two $\Delta B = 1$ effective couplings.

Employing an effective-theory language, what we mean under these two hypotheses is that the generic dimension-six operators encoding NP contributions to $B_d^0\text{--}\overline{B}_d^0$ and $\Delta B = 1$ transitions can be written as

$$Q_{\Delta B=2}^{\text{NP}} = \frac{\delta_{bd}^2}{\Lambda_{\text{eff}}^2} (\overline{b}\Gamma d)(\overline{b}\Gamma d), \quad Q_{\Delta B=1}^{\text{NP}} = \frac{\delta_{bd}}{\Lambda_{\text{eff}}^2} (\overline{b}\Gamma d)(\overline{q}\Gamma q), \quad (12)$$

where δ_{bd} denotes the new $\Delta B = 1$ effective flavour-changing coupling, Γ indicates generic Dirac and/or colour structures, and possible coefficient functions of $\mathcal{O}(1)$ have been ignored. Coherently with the requirement ii), we shall also assume that $(\text{SU}(2)_L \times \text{U}(1)_Y)$ -breaking operators of dimension less than six, such as the chromomagnetic operator, play a negligible role. The overall normalization of the two operators in (12), or the definition of the effective scale Λ_{eff} , has been chosen such that the corresponding SM $\Delta B = 2$ term is

$$Q_{\Delta B=2}^{\text{SM}} = \frac{(V_{tb}^* V_{td})^2}{M_W^2} (\overline{b}\Gamma d)(\overline{b}\Gamma d). \quad (13)$$

Choosing this normalization, we have implicitly factorized out an overall coefficient of $\mathcal{O}[(g/\sqrt{2})^4/(16\pi^2)]$ in the effective Hamiltonian, both in the $\Delta B = 2$ and in the $\Delta B = 1$

cases. As a result, within the SM, the loop-induced $\Delta B = 1$ operators can be written as

$$Q_{\Delta B=1}^{\text{SM}} = \mathcal{C} \frac{V_{tb}^* V_{td}}{M_W^2} (\bar{b}\Gamma d)(\bar{q}\Gamma q), \quad (14)$$

where the coefficient function \mathcal{C} is of $\mathcal{O}(1)$ in the case of pure short-distance-dominated electroweak operators (such as those generated by Z -penguin and W -box diagrams) and substantially larger than unity for those that receive large logarithmic corrections via RGE.

Note that the normalization of the NP contributions in (13) does not necessarily imply that they are generated only by loop amplitudes at the fundamental level: their natural size is comparable to that of SM loop amplitudes, but they could well be induced by tree-level processes. For instance, a model with a heavy Z' boson with a FCNC coupling to the $\bar{b}\Gamma d$ current would also perfectly fit in this scheme, and in this case *both* $Q_{\Delta B=1}^{\text{SM}}$ and $Q_{\Delta B=2}^{\text{SM}}$ would receive tree-level contributions. What we cannot accommodate in this scheme is the possibility that $Q_{\Delta B=1}^{\text{SM}}$ receives large tree-level contributions and $Q_{\Delta B=2}^{\text{SM}}$ only loop-induced ones: in our language, this case would correspond to a violation of the condition ii).

Since the measurement of the $B_d^0 - \overline{B}_d^0$ mass difference falls in the ballpark of the SM expectations, the new flavour-changing coupling δ_{bd} cannot be arbitrarily large: barring fine-tuned scenarios with severe cancellations among different terms, we can allow at most $\mathcal{O}(1)$ corrections to the SM amplitude. This implies (see also [7])

$$\frac{\langle Q_{\Delta B=2}^{\text{NP}} \rangle}{\langle Q_{\Delta B=2}^{\text{SM}} \rangle} \lesssim 1 \quad \rightarrow \quad \frac{\delta_{bd}}{\Lambda_{\text{eff}}} \lesssim \frac{V_{tb}^* V_{td}}{M_W}, \quad (15)$$

where possible $\mathcal{O}(1)$ factors associated with the matrix elements of the operators have been neglected.

Owing to the different parametric dependence from scale factor and flavour-changing coupling of $\Delta B = 2$ and $\Delta B = 1$ operators in (12), if the condition (15) is fulfilled the corresponding non-standard effects induced in $\Delta B = 1$ flavour-changing neutral-current transitions turn out to be suppressed at least by a factor $\mathcal{O}(M_W/\Lambda_{\text{eff}})$ relative to the SM level:

$$\frac{\langle Q_{\Delta B=2}^{\text{NP}} \rangle}{\langle Q_{\Delta B=2}^{\text{SM}} \rangle} \lesssim 1 \quad \rightarrow \quad \frac{\langle Q_{\Delta B=1}^{\text{NP}} \rangle}{\langle Q_{\Delta B=1}^{\text{SM}} \rangle} \leq \frac{1}{\mathcal{C}} \frac{M_W}{\Lambda_{\text{eff}}}. \quad (16)$$

Since the coefficient \mathcal{C} is substantially larger than 1 for QCD-penguin amplitudes, the suppression is even more severe in this case. We have thus obtained a natural justification for the smallness of non-standard effects in $\Delta B = 1$ loop-induced amplitudes in the well-motivated scenario of a heavy NP scale ($\Lambda_{\text{eff}} \gg M_W$).

Although rather qualitative, the above argument has the great advantage of being almost independent of the details of the NP model. Indeed, it can be realized in very different frameworks, from low-energy supersymmetry to models with large extra dimensions. As can be easily understood, this argument does not apply only to $B_d^0 - \overline{B}_d^0$ mixing: it is characteristic of any type of $\Delta F = 2$ meson-antimeson mixing versus the corresponding $\Delta F = 1$ loop-induced amplitudes, provided the corresponding assumption ii)

is fulfilled. For this reason, in the phenomenological determination of the CKM matrix of Section 4, we shall try to avoid the use of observables such as ε_K or ΔM_s , which are sensitive to the $K^0-\bar{K}^0$ and $B_s^0-\bar{B}_s^0$ mixing amplitudes, respectively.

In principle, the case of $b \rightarrow s$ transitions is somehow different from the $b \rightarrow d$ and $s \rightarrow d$ ones, since the $B_s^0-\bar{B}_s^0$ mass difference has not yet been measured. This is indeed one of the reasons why speculations about possible large NP effects in penguin-mediated $b \rightarrow s$ transitions, such as $B \rightarrow \pi K$ and – especially $B \rightarrow \phi K$ – are still very popular (see, for instance, [24] and references therein). However, we recall that the available data on ΔM_s already show a preference for this observable to be close to its SM expectation [4]. If we assume that NP effects in ΔM_s can be at most of $\mathcal{O}(1)$, we can accommodate large NP effects in $b \rightarrow s$ transitions only by means of violations of the conditions i) and ii) [25], or by fine-tuning. Therefore, in order to understand the consistency of our scenario, it will be very interesting to follow the evolution of future measurements of $B \rightarrow \pi K$ and $B \rightarrow \phi K$ decays. So far, the available data on the $B \rightarrow \pi K$ observables fall well into the SM-allowed regions in observable space [13]. In particular, they do not indicate any anomalous behaviour of the $B_d \rightarrow \pi^\mp K^\pm$ mode, which will be used in Section 4 to control the penguin effects in $B_d \rightarrow \pi^+\pi^-$.

To conclude this general discussion, it is worth stressing that this mechanism is not representative of all possible models with new sources of flavour mixing. As already mentioned, the condition ii) is not necessarily fulfilled. Moreover, a large hierarchy of matrix elements could invalidate the conditions (15) and (16). This happens, for instance, in supersymmetry with specific choices of the soft-breaking terms. However, as we shall discuss in the following, it is very natural to assume that this mechanism works also within supersymmetric models, so that the largest NP effects appear only in $\Delta F = 2$ amplitudes.

3.2 The Supersymmetry Case

Among specific extensions of the SM, low-energy supersymmetry is certainly one of the most interesting and well-motivated possibilities. In the absence of a MFV pattern for the soft-breaking terms, sizeable modifications of FCNC amplitudes are naturally expected within this framework, and the mass-insertion approximation provides a very efficient tool to describe them [26].

Supersymmetric contributions to $B_d^0-\bar{B}_d^0$ mixing have been widely discussed in the literature (see [9] and references therein), and there exist several possibilities to accommodate arbitrary values of ϕ_d^{NP} . For instance, we can simply adjust the coupling $\delta_{b_L d_L}^D$ (or, equivalently, $\delta_{b_R d_R}^D$) to produce the desired modification of $B_d^0-\bar{B}_d^0$ mixing via gluino-mediated box diagrams. In this case the sum of supersymmetric and SM contributions to $B_d^0-\bar{B}_d^0$ mixing can be written as

$$\Delta M_d e^{-i\phi_d} \propto \frac{G_F^2 M_W^2}{2\pi^2} \eta_B S_0(x_t) \langle \bar{B}_d^0 | (\bar{b}_L \gamma_\mu d_L) | B_d^0 \rangle \times \left\{ [V_{tb}^* V_{td}]^2 + \frac{\alpha_S (\tilde{M}_q)^2 \sin^4 \Theta_W M_W^2}{\alpha_{\text{e.m.}} (M_Z)^2 \tilde{M}_q^2} r_\eta \frac{F_0(x_{qg})}{S_0(x_t)} [\delta_{b_L d_L}^D]^2 \right\}, \quad (17)$$

where $S_0(x_t \equiv m_t^2/M_W^2)$ and η_B denote the initial condition and leading QCD corrections of the SM Wilson coefficient, respectively (see, e.g., [27]). The explicit expression for F_0 – the supersymmetric loop function depending on the ratio $x_{qg} \equiv \tilde{M}_q^2/\tilde{M}_g^2$ of squark and gluino masses – and the corresponding QCD correction factor r_η can be found in [9]. As a reference figure, note that $F_0(1)/S_0(x_t) = 1/27/S_0(x_t) \approx 0.015$, and that we can set, to a good approximation, $r_\eta \approx 1$.

Expression (17) provides a simple realization of the general scenario discussed in the previous subsection, with the adimensional effective flavour-changing coupling given by $\delta_{b_L d_L}^D$, and the effective NP scale given by

$$\Lambda_{\text{eff}}^{\text{SUSY}} = \frac{\alpha_{\text{e.m.}}(M_Z)\tilde{M}_q}{\alpha_S(\tilde{M}_q)\sin^2\Theta_W} \left| \frac{S_0(x_t)}{r_\eta F_0(x_{qg})} \right|^{1/2} \approx 1.4 \text{ TeV} \times \left(\frac{\tilde{M}_q}{0.5 \text{ TeV}} \right). \quad (18)$$

According to condition (15), corrections to $B_d^0-\overline{B}_d^0$ mixing of $\mathcal{O}(1)$ should be obtained for $|\delta_{b_L d_L}^D| \sim 0.1 \times (\tilde{M}_q/0.5 \text{ TeV})$: this expectation is fully confirmed by the detailed analysis of [9]. As pointed out in [8], since SM and supersymmetric loop functions have the same sign,³ $\delta_{b_L d_L}^D$ must have a large imaginary part if the SM term gives too large a ΔM_d , as in the case where the “true value” of γ lies in the second quadrant. Interestingly, as we shall see in the following section, this scenario is the favoured one for $\phi_d \sim 133^\circ$.

Owing to the general dimensional argument in (16), a supersymmetric framework with $\tilde{M}_q \gtrsim 0.5 \text{ TeV}$, where $|\delta_{b_L d_L}^D| \sim 0.1 \times (\tilde{M}_q/0.5 \text{ TeV})$ is the only new source of flavour-symmetry breaking, leads to negligible effects in $\Delta B = 1$ transitions. This can be explicitly verified by means of [29] in the case of electroweak penguin amplitudes of the type $b \rightarrow (s, d)\ell^+\ell^-$, or by means of [30] in the case of $s \rightarrow d\nu\bar{\nu}$ transitions. According to these analyses, if $\tilde{M}_q \gtrsim 0.5 \text{ TeV}$ and if we have only left–left mass insertions, the supersymmetric corrections to electroweak penguin amplitudes reach at most the level of a few per cent with respect to the SM contributions. These results are particularly important for the discussion of rare decays in Section 5: they show that it is perfectly conceivable to have a scenario where the NP corrections to $B_d^0-\overline{B}_d^0$ mixing are large, but the direct NP contributions to the rare decay amplitudes are negligible.

Within this framework, i.e. with heavy squark masses and non-standard sources of flavour-symmetry breaking induced only by left–left mass insertions, the relative impact of non-standard effects is even smaller for non-leptonic QCD-penguin amplitudes, such as those contributing to $B_d \rightarrow \pi^+\pi^-$ and $B_d \rightarrow \pi^\mp K^\pm$ decays. Indeed, in this case the SM contribution is substantially enhanced by the coupling constant and by large (infra-red) logarithms [31].

On the other hand, as already mentioned in the general discussion, we recall that this framework is not representative of all possible supersymmetric scenarios. For instance, it is well known that by means of flavour-non-diagonal A terms, i.e. mass insertions of the left–right type, we can generate sizeable effects in $\Delta F = 1$ transitions – in particular rare decays – without contradicting the $\Delta F = 2$ bounds [32]. This happens because we may generate by means of left–right mass insertions sizeable contributions to $(\text{SU}(2)_L \times \text{U}(1)_Y)$ -breaking $\Delta F = 1$ operators, which allow us to evade condition ii)

³This statement is not valid for arbitrary x_{qg} ; however, it holds for $x_{qg} \sim 1$, which is suggested by RGE constraints in grand-unified scenarios [28].

[33]. Similarly, condition ii) is badly violated by Higgs-mediated FCNC amplitudes in large $\tan\beta$ scenarios (see, in particular, [34]). Also in this case the reason is intimately related to an interplay between flavour- and electroweak-symmetry breaking [11].

To summarize, we can state that the scenario with large non-standard effects only in $\Delta F = 2$ amplitudes is characteristic of supersymmetric models with: i) a heavy scale for the soft-breaking terms, ii) new sources of flavour-symmetry breaking only (or mainly) in the soft-breaking terms which do not involve the Higgs fields, iii) Yukawa interactions very similar to the pure SM case.

4 Determination of the Unitarity Triangle

Let us now assume that we have NP of the kind specified in the previous section. We may then complement the experimentally determined B_d^0 - \overline{B}_d^0 mixing phase ϕ_d and the CKM factor R_b with data on CP violation in the B -factory benchmark mode $B_d \rightarrow \pi^+\pi^-$ to fix the apex of the “true” unitarity triangle in the $\overline{\rho}$ - $\overline{\eta}$ plane.

4.1 CP Violation in $B_d \rightarrow \pi^+\pi^-$

The decay $B_d^0 \rightarrow \pi^+\pi^-$ originates from $\overline{b} \rightarrow \overline{u}u\overline{d}$ quark-level transitions. Within the SM and the scenario for NP introduced in Section 3, we may write the corresponding decay amplitude as follows [22]:

$$A(B_d^0 \rightarrow \pi^+\pi^-) \propto [e^{i\gamma} - de^{i\theta}], \quad (19)$$

where the CP-conserving strong parameter $de^{i\theta}$ measures – sloppily speaking – the ratio of penguin to tree contributions in $B_d \rightarrow \pi^+\pi^-$. If we had negligible penguin contributions, i.e. $d = 0$, the corresponding CP-violating observables were simply given by

$$\mathcal{A}_{\text{CP}}^{\text{dir}}(B_d \rightarrow \pi^+\pi^-) = 0, \quad \mathcal{A}_{\text{CP}}^{\text{mix}}(B_d \rightarrow \pi^+\pi^-) = \sin(\phi_d + 2\gamma) \stackrel{\text{SM}}{=} -\sin 2\alpha, \quad (20)$$

where we have, in the last identity, also used the SM relation $\phi_d = 2\beta$ and the unitarity relation $2\beta + 2\gamma = 2\pi - 2\alpha$. We observe that actually the phases ϕ_d and γ enter directly in the $B_d \rightarrow \pi^+\pi^-$ observables, and not α . Consequently, since ϕ_d can be fixed straightforwardly through $B_d \rightarrow J/\psi K_S$, we may use $B_d \rightarrow \pi^+\pi^-$ to probe γ , which has important advantages when dealing with penguin and NP effects [13]. We shall come back to this point below.

Measurements of the CP-violating $B_d \rightarrow \pi^+\pi^-$ observables are already available:

$$\mathcal{A}_{\text{CP}}^{\text{dir}}(B_d \rightarrow \pi^+\pi^-) = \begin{cases} -0.30 \pm 0.25 \pm 0.04 & (\text{BaBar [35]}) \\ -0.77 \pm 0.27 \pm 0.08 & (\text{Belle [36]}) \end{cases} \quad (21)$$

$$\mathcal{A}_{\text{CP}}^{\text{mix}}(B_d \rightarrow \pi^+\pi^-) = \begin{cases} -0.02 \pm 0.34 \pm 0.05 & (\text{BaBar [35]}) \\ +1.23 \pm 0.41_{-0.08}^{+0.07} & (\text{Belle [36]}). \end{cases} \quad (22)$$

The BaBar and Belle results are unfortunately not fully consistent with each other. Hopefully, the experimental picture will be clarified soon. If we nevertheless form the

weighted averages of (21) and (22), using the rules of the Particle Data Group (PDG) [37], we obtain

$$\mathcal{A}_{\text{CP}}^{\text{dir}}(B_d \rightarrow \pi^+\pi^-) = -0.51 \pm 0.19 \quad (0.23) \quad (23)$$

$$\mathcal{A}_{\text{CP}}^{\text{mix}}(B_d \rightarrow \pi^+\pi^-) = +0.49 \pm 0.27 \quad (0.61), \quad (24)$$

where the errors in brackets are the ones increased by the PDG scaling-factor procedure. Direct CP violation at this level would require large penguin contributions with large CP-conserving strong phases. Interestingly, a significant impact of penguins on $B_d \rightarrow \pi^+\pi^-$ is also indicated by data on the $B \rightarrow \pi K, \pi\pi$ branching ratios [12, 13, 38], as well as by theoretical considerations [39, 40]. Consequently, it is already evident that the penguin contributions to $B_d \rightarrow \pi^+\pi^-$ *cannot* be neglected.

4.2 Complementing $B_d \rightarrow \pi^+\pi^-$ with $B_d \rightarrow \pi^\mp K^\pm$

Over the recent years, many approaches to control the impact of the penguin contributions on the extraction of weak phases from the CP-violating $B_d \rightarrow \pi^+\pi^-$ observables were proposed (see, for example, [38, 39, 41]). Let us here follow the method suggested in [12, 13], which is a variant of the $B_d \rightarrow \pi^+\pi^-, B_s \rightarrow K^+K^-$ strategy proposed in [22]. If we apply (19), we may write (for explicit expressions, see [22]):

$$\mathcal{A}_{\text{CP}}^{\text{dir}}(B_d \rightarrow \pi^+\pi^-) = \text{fct}(d, \theta, \gamma), \quad \mathcal{A}_{\text{CP}}^{\text{mix}}(B_d \rightarrow \pi^+\pi^-) = \text{fct}(d, \theta, \gamma, \phi_d), \quad (25)$$

which are *exact* parametrizations within the SM, and hold also for the NP scenario specified in Section 3. If we fix ϕ_d through (5), these two observables depend on three unknown parameters, d, θ and γ . In order to extract these quantities, it would be ideal to measure the following observables:

$$\mathcal{A}_{\text{CP}}^{\text{dir}}(B_s \rightarrow K^+K^-) = \text{fct}(d', \theta', \gamma), \quad \mathcal{A}_{\text{CP}}^{\text{mix}}(B_s \rightarrow K^+K^-) = \text{fct}(d', \theta', \gamma, \phi_s), \quad (26)$$

where ϕ_s can be assumed to be negligibly small in the SM, or can be fixed through CP-violating effects in $B_s \rightarrow J/\psi\phi$. Since $B_s \rightarrow K^+K^-$ is related to $B_d \rightarrow \pi^+\pi^-$ through an interchange of all strange and down quarks, i.e. through the U -spin flavour symmetry of strong interactions, we may derive the U -spin relation

$$d' = d, \quad (27)$$

which allows us to determine d, θ, θ' and γ from the CP-violating observables of the $B_s \rightarrow K^+K^-, B_d \rightarrow \pi^+\pi^-$ system [22]. Unfortunately, $B_s \rightarrow K^+K^-$ is not accessible at the e^+e^- B factories operating at the $\Upsilon(4S)$ resonance; this decay can be observed for the first time at run II of the Tevatron [42], and can be ideally studied in the era of the LHC [43]. However, since $B_s \rightarrow K^+K^-$ is related to $B_d \rightarrow \pi^\mp K^\pm$ through an interchange of spectator quarks, we may approximately use $B_d \rightarrow \pi^\mp K^\pm$, which has already been measured at the B factories, to deal with the penguins in $B_d \rightarrow \pi^+\pi^-$ [12]. The key quantity is then the following ratio of the CP-averaged $B_d \rightarrow \pi^+\pi^-$ and $B_d \rightarrow \pi^\mp K^\pm$ branching ratios:

$$H \equiv \frac{1}{\epsilon} \left(\frac{f_K}{f_\pi} \right)^2 \left[\frac{\text{BR}(B_d \rightarrow \pi^+\pi^-)}{\text{BR}(B_d \rightarrow \pi^\mp K^\pm)} \right] = \left\{ \begin{array}{l} 7.4 \pm 2.5 \text{ (CLEO [44])} \\ 7.6 \pm 1.2 \text{ (BaBar [45])} \\ 7.1 \pm 1.9 \text{ (Belle [46])}, \end{array} \right\} = 7.5 \pm 0.9, \quad (28)$$

where the factor f_K/f_π involving the kaon and pion decay constants takes into account factorizable U -spin-breaking corrections, and $\epsilon \equiv \lambda^2/(1-\lambda^2)$. If we employ – in addition to (27) – another U -spin relation,

$$\theta' = \theta, \quad (29)$$

and make plausible dynamical assumptions to replace the $B_s \rightarrow K^+K^-$ channel through $B_d \rightarrow \pi^\mp K^\pm$,⁴ we may write

$$H = \text{fct}(d, \theta, \gamma). \quad (30)$$

Consequently, (25) and (30) allow us now to determine γ , as well as d and θ . The explicit formulae to implement this strategy can be found in [13], taking also into account possible corrections to (27) and (29). As pointed out in [13, 47], there is a transparent way to characterize the $B_d \rightarrow \pi^+\pi^-$ mode in the space of its CP-violating observables, allowing a simple comparison with the experimental data. Let us focus here on the unitarity triangle and the allowed region for its apex in the $\bar{\rho}-\bar{\eta}$ plane.

4.3 Fixing the Apex of the Unitarity Triangle

If we follow [13] and employ the quantity H to control the penguin effects in $B_d \rightarrow \pi^+\pi^-$, we may convert the direct and mixing-induced CP asymmetries of this decay into values of γ . Using $H = 7.5$ and the experimental averages given in (23) and (24), we obtain

$$35^\circ \lesssim \gamma \lesssim 79^\circ (\phi_d = 47^\circ), \quad 101^\circ \lesssim \gamma \lesssim 145^\circ (\phi_d = 133^\circ). \quad (31)$$

As pointed out in [13], these solutions are related to each other through

$$\phi_d \rightarrow 180^\circ - \phi_d, \quad \gamma \rightarrow 180^\circ - \gamma. \quad (32)$$

Because of the unsatisfactory experimental situation concerning the CP asymmetries of $B_d \rightarrow \pi^+\pi^-$, the ranges in (31) should mainly be considered as an illustration of how our strategy is working. Indeed, in order to obtain (31), we have just used the “ordinary” errors in (23) and (24), and not the enlarged ones given there in brackets. Interestingly, the information on the *positive* sign of $\mathcal{A}_{\text{CP}}^{\text{mix}}(B_d \rightarrow \pi^+\pi^-)$, which is favoured by the Belle measurement [36], already implies that $\gamma \sim 60^\circ$ *cannot* be accommodated in the case of $\phi_d \sim 133^\circ$, as emphasized in [13]. The experimental uncertainties will be reduced considerably in the future, thereby providing significantly more stringent results for γ .

It should be noted that we have assumed in (31) – as is usually done – that $\gamma \in [0^\circ, 180^\circ]$. This range is implied by the interpretation of ε_K , provided that: i) NP does not change the sign of the $\Delta S = 2$ amplitude with respect to the SM; ii) the “bag” parameter B_K is positive (as indicated by all existing non-perturbative calculations). A similar assumption about the “bag” parameter B_{B_q} – the B_q -meson counterpart of B_K – enters also in (2); for a discussion of the very unlikely $B_K < 0$, $B_{B_q} < 0$ cases, see [48]. If we relaxed these assumptions about NP and/or “bag” parameters, we would need to double the solutions and consider the specular case $\gamma \in [180^\circ, 360^\circ]$.

Using (31), we may now fix the apex of the unitarity triangle. To this end, we insert (31) into (11), and use the range for R_b given in (7). The results of this exercise are

⁴Note that the U -spin relation (27) is sufficient in the case of the $B_s \rightarrow K^+K^-$, $B_d \rightarrow \pi^+\pi^-$ strategy.

Experimental data	Hadronic parameters
$\lambda = 0.2241 \pm 0.0036$	$\bar{B}_K = 0.85 \pm 0.15$
$ V_{cb} = 0.041 \pm 0.002$	$f_{B_d} \sqrt{\hat{B}_{B_d}} = (230 \pm 28 \pm 28) \text{ MeV}$
$R_b = 0.38 \pm 0.08$	$f_{B_d} = (203 \pm 27_{-20}^0) \text{ MeV}$
$\overline{m}_t(m_t) = (167 \pm 5) \text{ GeV}$	$f_{B_s} = (238 \pm 31) \text{ MeV}$
$\Delta M_d = (0.503 \pm 0.006) \text{ ps}^{-1}$	$\xi = 1.16$
$\Delta M_s > 14.4 \text{ ps}^{-1}$	

Table 1: Input values used to draw the ε_K , ΔM_d and $\Delta M_s/\Delta M_d$ constraints in Figs. 2 and 3, and to analyse the branching ratios of rare decays in Section 5. As usual, we define $\xi \equiv (f_{B_s}/f_{B_d})\sqrt{\hat{B}_{B_s}/\hat{B}_{B_d}}$.

shown in Figs. 2 and 3 for $\phi_d = 47^\circ$ and $\phi_d = 133^\circ$, respectively. Because of (32), the values of $\bar{\rho}$ and $\bar{\eta}$ corresponding to these two solutions for ϕ_d are related to each other as follows:

$$\bar{\rho} \rightarrow -\bar{\rho}, \quad \bar{\eta} \rightarrow \bar{\eta}. \quad (33)$$

In order to guide the eye, we have also included in Figs. 2 and 3 the well-known SM ε_K hyperbola. In Fig. 2, we show also the $\beta = 23.5^\circ$ branch, which corresponds to the SM interpretation of $\phi_d = 47^\circ$, as well as the circle with radius R_t around $(1, 0)$ that is fixed through ΔM_d , and the constraint arising from the lower bound on $\Delta M_s/\Delta M_d$. In order to draw the SM $\Delta M_{d,s}$ contours, as well as the one implied by ε_K ,⁵ we use the parameters collected in Table 1, which will also be employed in the discussion of rare decays in Section 5. It is remarkable that we obtain a perfect agreement of our $B_d \rightarrow \pi^+\pi^-$ range, which does *not* rely on ε_K or $B_d^0-\overline{B}_d^0$ mixing, with *all* these constraints. On the other hand, the case of $\phi_d = 133^\circ$ shown in Fig. 3 requires large NP contributions to $B_d^0-\overline{B}_d^0$ mixing, so that we may there *no longer* use ΔM_d or $\Delta M_s/\Delta M_d$ to determine the side R_t of the unitarity triangle, and may *no longer* convert ϕ_d directly into a straight line in the $\bar{\rho}-\bar{\eta}$ plane. For this reason, we have not included the corresponding contours in Fig. 3. Interestingly, our $\phi_d = 133^\circ$ region would still be consistent with the ε_K hyperbola, but would now favour values of γ that are larger than 90° . The difference between the black range in this figure and the $\phi_d \sim 133^\circ$ branch illustrated in Fig. 1(b), which is usually used in the literature to represent this case, is striking. As we have already emphasized, once we agree that the value of R_b cannot be modified by NP effects, it is *not* correct to include this branch in the $\bar{\rho}-\bar{\eta}$ plane.

The results shown in Figs. 2 and 3 are complemented by Table 2, where we collect the ranges for the angles α , β and γ of the unitarity triangle, as well as those for the generalized Wolfenstein parameters $\bar{\rho}$ and $\bar{\eta}$. In this table, we illustrate also the impact of U -spin-breaking effects on (27), which are described by the following parameter:

$$\tilde{\xi} = d'/d. \quad (34)$$

⁵We recall that these constraints are only shown for illustrative purposes, and are not used to fix the allowed region in the $\bar{\rho}-\bar{\eta}$ plane.

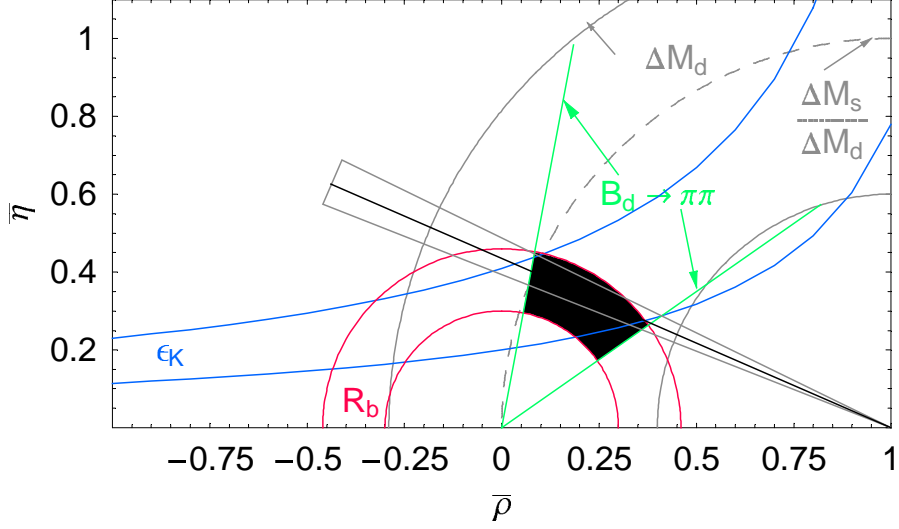


Figure 2: Allowed region for the apex of the unitarity triangle determined from the CP-violating $B_d \rightarrow \pi^+\pi^-$ observables given in (23) and (24) in the case of $\phi_d = 47^\circ$ ($H = 7.5$). For comparison, we also show the hyperbola corresponding to the SM interpretation of ϵ_K , the $\beta = 23.5^\circ$ branch arising from the SM interpretation of ϕ_d , the circle corresponding to the SM interpretation of ΔM_d (solid grey), and the upper bound on R_t (dashed grey), which originates from the lower bound on ΔM_s (see Table 1).

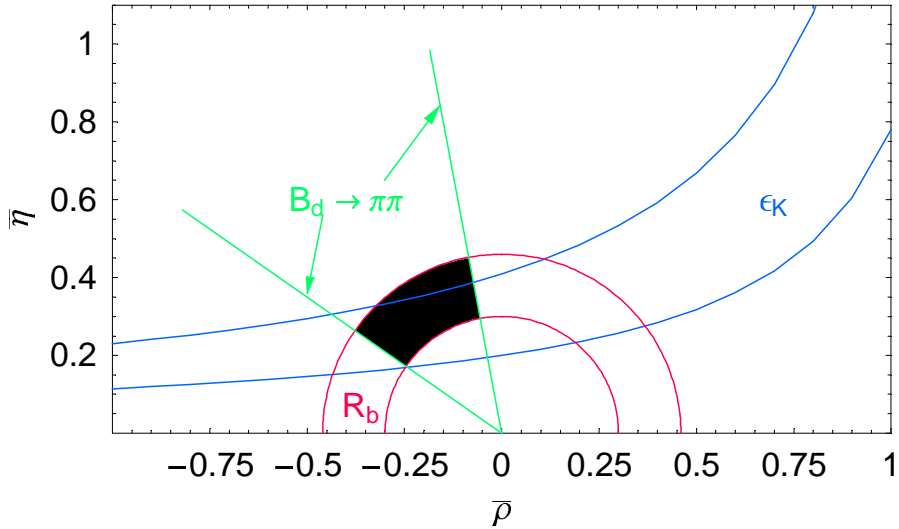


Figure 3: Allowed region for the apex of the unitarity triangle determined from the CP-violating $B_d \rightarrow \pi^+\pi^-$ observables given in (23) and (24) in the case of $\phi_d = 133^\circ$ ($H = 7.5$). The hyperbola corresponds to the SM interpretation of ϵ_K .

As noted in [13], these effects are potentially much more important than possible corrections to (29). Nevertheless, we observe that the impact of a variation of ξ within $[0.8, 1.2]$ is quite moderate. Interestingly, we may well accommodate values of α around 90° in the case of $\phi_d = 47^\circ$, in contrast to the situation of $\phi_d = 133^\circ$, which would favour α to lie around 40° . Theoretical arguments for $\alpha \sim 90^\circ$ were given in [49].

Let us now compare our results with the analysis performed by the Belle collaboration in [36], yielding the range

$$78^\circ \leq \phi_2 \equiv \alpha \leq 152^\circ. \quad (35)$$

The starting point of this study, which follows closely [38], is also the parametrization (19) of the $B_d^0 \rightarrow \pi^+\pi^-$ decay amplitude. However, there are important differences in comparison with our analysis:

- i) The range in (35) corresponds to the 95.5% C.L. interval of the Belle asymmetries, constrained to lie within the physical region, whereas the results in Table 2 were obtained for the averages of the BaBar and Belle measurements in (23) and (24) (with “ordinary” errors), which fall well into the 95.5% C.L. Belle region.
- ii) In the Belle analysis, d was varied within $[0.15, 0.45]$ to explore the penguin effects, whereas we use the observable H to control the penguin contributions.
- iii) A crucial difference arises, since the SM relation $\phi_d = 2\beta$ was used in [36], in combination with the unitarity relation $\beta + \gamma = \pi - \alpha$, to eliminate γ (see (20)). Following these lines, the attention is implicitly restricted to the standard solution $\phi_d = 47^\circ$ with $\beta = 23.5^\circ$, so that the case of $\phi_d = 133^\circ$ *cannot* be explored.

Despite the different input values for the CP asymmetries and the different treatment of the penguin contributions, (35) is in good agreement with the ranges for α collected in Table 2 for $\phi_d = 47^\circ$.⁶ On the other hand, all the interesting features related to the $\phi_d = 133^\circ$ solution were not addressed in the analysis in [36].

4.4 Further Implications from $B \rightarrow \pi\pi, \pi K$

Interestingly, flavour-symmetry strategies to determine γ with the help of charged [50] and neutral [51] $B \rightarrow \pi K$ modes show some preference for values of γ larger than 90° (for recent overviews, see [52]). Moreover, as pointed out in [12, 13], the theoretical predictions for the penguin parameter $de^{i\theta}$ obtained within the “QCD factorization” [39] and “PQCD” [40] approaches can be brought to better agreement with the measured value of H in the case of $\gamma > 90^\circ$. It should also be noted that the global fits to all available $B \rightarrow \pi K, \pi\pi$ data show a similar picture (see, for instance, [39, 53]). Since the $B \rightarrow \pi K$ analyses are rather involved, we shall not discuss them here in further detail; let us just emphasize that their preferred values for γ could be conveniently accommodated in Fig. 3, i.e. for $\phi_d = 133^\circ$, but not in the case of the conventional $\phi_d = 47^\circ$ solution shown in Fig. 2. Because of the large experimental uncertainties, it is of course too early to draw definite conclusions, but the experimental situation is expected to improve

⁶If we assume $\beta = 23.5^\circ$ and insert the $\phi_d = 47^\circ$ range for γ in (31) into $\alpha = 180^\circ - \beta - \gamma$, we obtain $78^\circ \lesssim \alpha \lesssim 122^\circ$. As (35), this range does not depend on R_b , but relies on the SM relation $\phi_d = 2\beta$.

Case of $\tilde{\xi} = 1$	α	β	γ	$\bar{\rho}$	$\bar{\eta}$
$\phi_d = 47^\circ$	$(103 \pm 29)^\circ$	$(20 \pm 7)^\circ$	$(57 \pm 22)^\circ$	$+0.21 \pm 0.16$	$+0.31 \pm 0.14$
$\phi_d = 133^\circ$	$(44 \pm 20)^\circ$	$(15 \pm 7)^\circ$	$(123 \pm 22)^\circ$	-0.21 ± 0.16	$+0.31 \pm 0.14$
Case of $\tilde{\xi} = 0.8$	α	β	γ	$\bar{\rho}$	$\bar{\eta}$
$\phi_d = 47^\circ$	$(102 \pm 33)^\circ$	$(19 \pm 8)^\circ$	$(59 \pm 26)^\circ$	$+0.20 \pm 0.18$	$+0.31 \pm 0.15$
$\phi_d = 133^\circ$	$(46 \pm 23)^\circ$	$(16 \pm 8)^\circ$	$(121 \pm 26)^\circ$	-0.20 ± 0.18	$+0.31 \pm 0.15$
Case of $\tilde{\xi} = 1.2$	α	β	γ	$\bar{\rho}$	$\bar{\eta}$
$\phi_d = 47^\circ$	$(104 \pm 26)^\circ$	$(20 \pm 7)^\circ$	$(56 \pm 19)^\circ$	$+0.22 \pm 0.14$	$+0.31 \pm 0.13$
$\phi_d = 133^\circ$	$(43 \pm 17)^\circ$	$(15 \pm 7)^\circ$	$(124 \pm 19)^\circ$	-0.22 ± 0.14	$+0.31 \pm 0.13$

Table 2: The ranges for the angles of the unitarity triangle and the generalized Wolfenstein parameters corresponding to the black regions shown in Figs. 2 and 3 ($\tilde{\xi} = 1$). In order to illustrate the impact of possible U -spin breaking effects (see (34)), we give also the ranges arising for $\tilde{\xi} = 0.8$ and $\tilde{\xi} = 1.2$. Note that the values for $\bar{\rho}$ and $\bar{\eta}$ satisfy (33).

continuously in the future. In this context, it is also helpful to construct a set of robust sum rules [54], which are satisfied by the $B \rightarrow \pi K$ observables.

5 Implications for $K \rightarrow \pi \nu \bar{\nu}$ and $B_{d,s} \rightarrow \mu^+ \mu^-$

In this section, we shall explore the implications of the allowed regions in the $\bar{\rho}$ - $\bar{\eta}$ plane shown in Figs. 2 and 3 for the branching ratios of the very rare decay processes $K \rightarrow \pi \nu \bar{\nu}$ and $B_{d,s} \rightarrow \mu^+ \mu^-$. Needless to note, the predictions corresponding to the $\phi_d = 133^\circ$ scenario are of particular interest. As in the previous section, we assume that NP does not affect the amplitudes of these modes, i.e. that it manifests itself only through the different allowed ranges for $\bar{\rho}$ and $\bar{\eta}$ shown in Figs. 2 and 3.

5.1 $K \rightarrow \pi \nu \bar{\nu}$

As is well known, the rare kaon decays $K^+ \rightarrow \pi^+ \nu \bar{\nu}$ and $K_L \rightarrow \pi^0 \nu \bar{\nu}$ offer valuable tools to explore flavour physics. These modes originate from Z penguins and box diagrams, and are theoretically very clean. Let us first focus on $K^+ \rightarrow \pi^+ \nu \bar{\nu}$, which has already been observed by the E787 experiment at BNL through two clean events, yielding the following branching ratio [55]:

$$\text{BR}(K^+ \rightarrow \pi^+ \nu \bar{\nu}) = (1.57_{-0.82}^{+1.75}) \times 10^{-10}. \quad (36)$$

Within the SM and the NP scenarios specified above, the “reduced” branching ratio [56]

$$B_1 = \frac{\text{BR}(K^+ \rightarrow \pi^+ \nu \bar{\nu})}{4.42 \times 10^{-11}} \quad (37)$$

takes the following form:

$$B_1 = \left[\frac{\text{Im}\lambda_t}{\lambda^5} X(x_t) \right]^2 + \left[\frac{\text{Re}\lambda_t}{\lambda^5} X(x_t) + \frac{\text{Re}\lambda_c}{\lambda} P_c(\nu \bar{\nu}) \right]^2, \quad (38)$$

where $X(x_t) = 1.51 \pm 0.05$ and $P_c(\nu\bar{\nu}) = 0.40 \pm 0.06$ are appropriate coefficient functions, which encode top- and charm-quark loop contributions, respectively [57]. Taking into account $\lambda_t \equiv V_{ts}^* V_{td}$ and $\lambda_c \equiv V_{cs}^* V_{cd}$, we obtain

$$\text{Im}\lambda_t = \eta A^2 \lambda^5, \quad \text{Re}\lambda_t = -\left(1 - \frac{\lambda^2}{2}\right) A^2 \lambda^5 (1 - \bar{\rho}) \quad (39)$$

and

$$\text{Re}\lambda_c = -\lambda \left(1 - \frac{\lambda^2}{2}\right), \quad (40)$$

respectively, where $A \equiv |V_{cb}|/\lambda^2$.

The following ranges for the $K^+ \rightarrow \pi^+ \nu\bar{\nu}$ branching ratio are obtained by scanning $\bar{\rho}$ and $\bar{\eta}$ within the black regions shown in Figs. 2 and 3, and varying simultaneously $X(x_t)$, P_c and the relevant parameters in Table 1 within their allowed ranges. In the case when $\phi_d = 47^\circ$, we obtain

$$0.33 \times 10^{-10} \leq \text{BR}(K^+ \rightarrow \pi^+ \nu\bar{\nu}) \leq 1.19 \times 10^{-10}, \quad (41)$$

whereas the $\phi_d = 133^\circ$ scenario favours a larger branching ratio,

$$0.65 \times 10^{-10} \leq \text{BR}(K^+ \rightarrow \pi^+ \nu\bar{\nu}) \leq 1.97 \times 10^{-10}, \quad (42)$$

which is due to the sign-change of $\bar{\rho}$ in (33). Despite the large present uncertainties, it is interesting to note that (42) is in better agreement with the experimental result (36), thereby favouring the $\phi_d = 133^\circ$ solution. On the other hand, (41) agrees well with the SM range

$$\text{BR}(K^+ \rightarrow \pi^+ \nu\bar{\nu}) = (0.72 \pm 0.21) \times 10^{-10} \quad (43)$$

given in [8], which is not surprising. Note, however, that (41) relies only on the data on ϕ_d , CP violation in $B_d \rightarrow \pi^+ \pi^-$, the observable H , and the measurement of the side R_b of the unitarity triangle. On the other hand, the usual CKM fits were used in (43).

The observation that the central value of the BNL-E787 result does not necessarily imply a non-standard contribution to the $K^+ \rightarrow \pi^+ \nu\bar{\nu}$ amplitude, but that it could well be accommodated by NP effects in $B_d^0 - \bar{B}_d^0$ mixing only, has already been made in [8]. Indeed, the SM interpretation of the measured $\text{BR}(K^+ \rightarrow \pi^+ \nu\bar{\nu})$ defines a region in the $\bar{\rho}-\bar{\eta}$ plane which is perfectly consistent with the R_b circle, but favours $\gamma > 90^\circ$. Adding to this analysis the $B_d \rightarrow \pi^+ \pi^-$ information, we can now conclude that the measured $\text{BR}(K^+ \rightarrow \pi^+ \nu\bar{\nu})$ favours a $B_d^0 - \bar{B}_d^0$ mixing phase of $\phi_d = 133^\circ$.

Let us now have a brief look at the decay $K_L \rightarrow \pi^0 \nu\bar{\nu}$, which is characterized by

$$B_2 = \frac{\text{BR}(K_L \rightarrow \pi^0 \nu\bar{\nu})}{1.93 \times 10^{-10}}, \quad (44)$$

with

$$B_2 = \left[\frac{\text{Im}\lambda_t}{\lambda^5} X(x_t) \right]^2 = \eta^2 A^4 X(x_t)^2. \quad (45)$$

In contrast to B_1 , this reduced branching ratio does not depend on $\bar{\rho}$. Consequently, since the allowed ranges for $\bar{\eta}$ are equal in Figs. 2 and 3 because of (33), $K_L \rightarrow \pi^0 \nu\bar{\nu}$

does not allow us to distinguish between these two cases, i.e. we obtain the same range for $\phi_d = 47^\circ$ and 133° :

$$0.4 \times 10^{-11} \leq \text{BR}(K_L \rightarrow \pi^0 \nu \bar{\nu}) \leq 6.2 \times 10^{-11}, \quad (46)$$

which overlaps well with the SM expectation [58]

$$\text{BR}(K^+ \rightarrow \pi^+ \nu \bar{\nu}) = (2.8 \pm 1.0) \times 10^{-11}. \quad (47)$$

5.2 $B_{d,s} \rightarrow \mu^+ \mu^-$

Let us now, finally, turn to two rare B decays, $B_d \rightarrow \mu^+ \mu^-$ and $B_s \rightarrow \mu^+ \mu^-$. Within the SM and the kind of NP specified above, they are mediated by box diagrams and Z penguins. We may write the branching ratio for $B_d \rightarrow \mu^+ \mu^-$ as follows [59]:

$$\text{BR}(B_d \rightarrow \mu^+ \mu^-) = 1.1 \times 10^{-10} \left[\frac{f_{B_d}}{0.20 \text{ GeV}} \right]^2 \left[\frac{|V_{td}|}{0.008} \right]^2 \left[\frac{\tau_{B_d}}{1.5 \text{ ps}} \right] \left[\frac{\bar{m}_t(m_t)}{167 \text{ GeV}} \right]^{3.12}, \quad (48)$$

where $|V_{td}|^2$ is given by

$$|V_{td}|^2 = A^2 \lambda^6 R_t^2 = A^2 \lambda^6 [(1 - \bar{\rho})^2 + \bar{\eta}^2]. \quad (49)$$

We may now calculate, in analogy to our discussion of the $K \rightarrow \pi \nu \bar{\nu}$ modes given in Subsection 5.1, the range for this branching ratio corresponding to the black regions shown in Figs. 2 and 3. In the case of $\phi_d = 47^\circ$, we obtain

$$0.4 \times 10^{-10} \leq \text{BR}(B_d \rightarrow \mu^+ \mu^-) \leq 2.2 \times 10^{-10}, \quad (50)$$

whereas the $\phi_d = 133^\circ$ scenario favours the following, larger branching ratio:

$$1.2 \times 10^{-10} \leq \text{BR}(B_d \rightarrow \mu^+ \mu^-) \leq 4.2 \times 10^{-10}. \quad (51)$$

As in the case of $K^+ \rightarrow \pi^+ \nu \bar{\nu}$, the enhancement is due to the sign-change of $\bar{\rho}$ in (33).

On the other hand, we have

$$\text{BR}(B_s \rightarrow \mu^+ \mu^-) = 4.1 \times 10^{-9} \left[\frac{f_{B_s}}{0.24 \text{ GeV}} \right]^2 \left[\frac{|V_{ts}|}{0.040} \right]^2 \left[\frac{\tau_{B_s}}{1.5 \text{ ps}} \right] \left[\frac{\bar{m}_t(m_t)}{167 \text{ GeV}} \right]^{3.12}, \quad (52)$$

where V_{ts} is given – up to tiny corrections entering at the λ^4 level – as follows:

$$V_{ts} = -A\lambda^2 = -V_{cb}. \quad (53)$$

Consequently, since $\text{BR}(B_s \rightarrow \mu^+ \mu^-)$ does not depend on $\bar{\rho}$ and $\bar{\eta}$, if we neglect these corrections, it has no sensitivity on the allowed ranges in the $\bar{\rho}$ - $\bar{\eta}$ plane shown in Figs. 2 and 3, i.e. we obtain the same prediction for $\phi_d = 47^\circ$ and $\phi_d = 133^\circ$:

$$3.0 \times 10^{-9} \leq \text{BR}(B_s \rightarrow \mu^+ \mu^-) \leq 6.0 \times 10^{-9}. \quad (54)$$

At first sight, $\text{BR}(B_s \rightarrow \mu^+ \mu^-)$ does therefore not appear to be of great interest for our analysis. However, this is actually not the case, since the ratio

$$\frac{\text{BR}(B_d \rightarrow \mu^+ \mu^-)}{\text{BR}(B_s \rightarrow \mu^+ \mu^-)} = \left[\frac{\tau_{Bd}}{\tau_{Bs}} \right] \left[\frac{M_{Bd}}{M_{Bs}} \right] \left[\frac{f_{Bd}}{f_{Bs}} \right]^2 \left| \frac{V_{td}}{V_{ts}} \right|^2 \quad (55)$$

is affected to a much smaller extent by the hadronic uncertainties associated with f_{B_d} and f_{B_s} than the individual branching ratios. These decay constants now enter in a ratio, which equals 1 in the $SU(3)$ limit, i.e. we have only to deal with the $SU(3)$ -breaking corrections to this quantity [60]:

$$\frac{f_{B_s}}{f_{B_d}} = 1.18(4)_{-0}^{+12}, \quad (56)$$

whereas the ranges for the individual decay constants can be found in Table 1. Using (53) and taking (3) into account, we obtain from (55) the following expression:

$$R \equiv \left[\frac{\tau_{Bs}}{\tau_{Bd}} \right] \left[\frac{M_{Bs}}{M_{Bd}} \right] \left[\frac{f_{Bs}}{f_{Bd}} \right]^2 \left[\frac{\text{BR}(B_d \rightarrow \mu^+ \mu^-)}{\text{BR}(B_s \rightarrow \mu^+ \mu^-)} \right] = \lambda^2 R_t^2. \quad (57)$$

Since the side R_t of the unitarity triangle takes quite different values for the situations shown in Figs. 2 and 3 because of (33), we may nicely probe them through R . In the case of $\phi_d = 47^\circ$, we find

$$2.2 \times 10^{-2} \leq R \leq 5.4 \times 10^{-2}, \quad (58)$$

while our $\phi_d = 133^\circ$ scenario corresponds to

$$5.7 \times 10^{-2} \leq R \leq 10.1 \times 10^{-2}. \quad (59)$$

Unfortunately, the sensitivity of the existing experiments is still far from the level necessary to probe the ratio R . The present experimental upper bounds read as follows:

$$\text{BR}(B_s \rightarrow \mu^+ \mu^-) < 2.6 \times 10^{-6} \quad (95\% \text{ C.L. [61]}) \quad (60)$$

$$\text{BR}(B_d \rightarrow \mu^+ \mu^-) < 2.0 \times 10^{-7} \quad (90\% \text{ C.L. [62]}). \quad (61)$$

However, owing to clean experimental signatures, these processes are among the benchmark modes of future B -physics experiments at hadron colliders.

6 Conclusions and Outlook

The main points of this paper can be summarized as follows:

- We have emphasized that the CP-violating $B_d^0 - \overline{B}_d^0$ mixing phase $\phi_d \sim 47^\circ \vee 133^\circ$, which has been determined from $\mathcal{A}_{\text{CP}}^{\text{mix}}(B_d \rightarrow J/\psi K_S)$, cannot be represented straightforwardly in the $\overline{\rho} - \overline{\eta}$ plane in the presence of NP contributions to $B_d^0 - \overline{B}_d^0$ mixing. This feature affects in particular the “unconventional” solution of $\phi_d = 133^\circ$, which definitely requires such kind of physics beyond the SM. We have pointed out that it is therefore *not* correct to represent this solution simply as a second branch in the $\overline{\rho} - \overline{\eta}$ plane, as is usually done in the literature.

- In the solution of this problem, R_b and γ play a key rôle. From a theoretical point of view, certain pure tree decays, for example $B_d \rightarrow DK_S$ or $B_s \rightarrow D\phi$ modes, would offer an ideal tool to determine γ , providing theoretically clean results that are, in addition, very robust under the influence of NP. Unfortunately, these strategies cannot yet be implemented. However, an interesting alternative is offered by the B -factory benchmark mode $B_d \rightarrow \pi^+\pi^-$, where first experimental results on CP-violating effects are already available from BaBar and Belle.
- We have considered a specific scenario for physics beyond the SM, where we have large NP contributions to $B_d^0-\overline{B}_d^0$ mixing, but not to the $\Delta B = 1$ and $\Delta S = 1$ decay processes. Within this framework, we may then also straightforwardly accommodate the $\phi_d = 133^\circ$ solution. We have given general conditions for such a kind of NP, and have argued that it is well motivated in supersymmetry and several specific frameworks.
- We have pointed out that the CP-violating $B_d \rightarrow \pi^+\pi^-$ observables allow us to determine the “true” apex of the unitarity triangle for such a scenario of NP. In order to control the penguin effects, which definitely has to be done, we employ the CP-averaged $B_d \rightarrow \pi^\pm K^\mp$ branching ratio, and make use of U -spin and plausible dynamical assumptions. Following these lines, we may determine γ for each of the two solutions for ϕ_d . Complementing this information with the experimental range for R_b , we may fix the apex of the unitarity triangle, and thus determine also α and β . In the case of $\phi_d \sim 47^\circ$, we arrive at the first quadrant of the $\overline{\rho}-\overline{\eta}$ plane, and obtain an allowed region, which is in perfect agreement with the constraints arising from the SM interpretation of ϕ_d , ΔM_d and $\Delta M_s/\Delta M_d$, as well as of ε_K . On the other hand, for $\phi_d \sim 133^\circ$, we obtain an allowed region in the second quadrant, corresponding to $\gamma > 90^\circ$. Interestingly, this range is still consistent with the ε_K hyperbola, whereas we may now no longer use ΔM_d and $\Delta M_s/\Delta M_d$ to determine R_t , as these quantities would receive NP contributions.
- We have also explored the implications of these two solutions for very rare K and B decays, $K \rightarrow \pi\nu\overline{\nu}$ and $B_{d,s} \rightarrow \mu^+\mu^-$, respectively, assuming that their decay amplitudes take the same form as in the SM. In this case, NP would manifest itself only indirectly, through the determination of $\overline{\rho}$ and $\overline{\eta}$. Consequently, for $\phi_d = 47^\circ$ we obtain the same picture for these modes as in the SM. However, in the case of $\phi_d \sim 133^\circ$, the branching ratio for $K^+ \rightarrow \pi^+\nu\overline{\nu}$ that would be favoured is about twice as large as in the SM, and would be in better agreement with the present measurement. Similarly, if $\phi_d \sim 133^\circ$, a branching ratio about twice as large as in the SM is expected for $B_d \rightarrow \mu^+\mu^-$. On the other hand, the impact of this non-standard solution on both $\text{BR}(B_s \rightarrow \mu^+\mu^-)$ and $\text{BR}(K_L \rightarrow \pi^0\nu\overline{\nu})$ would be negligible.

At the present stage, we may not yet draw any definite conclusion, because of the large experimental uncertainties and the unsatisfactory situation of the measurement of the CP-violating $B_d \rightarrow \pi^+\pi^-$ observables; hopefully, the discrepancy between BaBar and Belle will be resolved soon. Interestingly, alternative analyses of the data for the $B \rightarrow$

$\pi K, \pi\pi$ branching ratios show some preference for $\gamma > 90^\circ$, thereby favouring the $\phi_d = 133^\circ$ scenario. A similar comment applies to the rare kaon decay $K^+ \rightarrow \pi^+ \nu \bar{\nu}$. On the other hand, it should not be forgotten that the allowed region for $\phi_d = 47^\circ$ is consistent with the stringent constraints from $B_{d,s}^0 - \overline{B}_{d,s}^0$ mixing. As far as ε_K is concerned, both the $\phi_d = 47^\circ$ and the $\phi_d = 133^\circ$ scenario are consistent with the SM interpretation of this quantity. In view of these observations, it would be very important to distinguish directly between the two solutions for ϕ_d , which are implied by their extraction from $\sin \phi_d$, through a measurement of the sign of $\cos \phi_d$.

Acknowledgements

J.M. acknowledges financial support by MCyT and FEDER FPA2002-00748. The work by G.I. and J.M. is partially supported by IHP-RTN, EC contract No. HPRN-CT-2002-00311 (EURIDICE).

References

- [1] M. Kobayashi and T. Maskawa, *Prog. Theor. Phys.* **49** (1973) 652.
- [2] BaBar Collaboration (B. Aubert *et al.*), *Phys. Rev. Lett.* **87** (2001) 091801;
Belle Collaboration (K. Abe *et al.*), *Phys. Rev. Lett.* **87** (2001) 091802.
- [3] L. Wolfenstein, *Phys. Rev. Lett.* **51** (1983) 1945;
A.J. Buras, M.E. Lautenbacher and G. Ostermaier, *Phys. Rev.* **D50** (1994) 3433.
- [4] A.J. Buras, TUM-HEP-435-01 [hep-ph/0109197];
A. Ali and D. London, *Eur. Phys. J.* **C18** (2001) 665;
D. Atwood and A. Soni, *Phys. Lett.* **B508** (2001) 17;
M. Ciuchini *et al.*, *JHEP* **0107** (2001) 013;
A. Höcker *et al.*, *Eur. Phys. J.* **C21** (2001) 225.
- [5] Y. Nir, WIS-35-02-DPP [hep-ph/0208080].
- [6] R. Fleischer, *Phys. Rep.* **370** (2002) 537.
- [7] R. Fleischer and T. Mannel, *Phys. Lett.* **B506** (2001) 311.
- [8] G. D'Ambrosio and G. Isidori, *Phys. Lett.* **B530** (2002) 108.
- [9] D. Becirevic *et al.*, *Nucl. Phys.* **B634** (2002) 105.
- [10] A.J. Buras *et al.*, *Phys. Lett.* **B500** (2001) 161.
- [11] G. D'Ambrosio, G.F. Giudice, G. Isidori and A. Strumia, *Nucl. Phys.* **B645** (2002) 155.
- [12] R. Fleischer, *Eur. Phys. J.* **C16** (2000) 87.
- [13] R. Fleischer and J. Matias, *Phys. Rev.* **D66** (2002) 054009.

- [14] Y. Grossman, Y. Nir and M.P. Worah, *Phys. Lett.* **B407** (1997) 307;
A.L. Kagan and M. Neubert, *Phys. Lett.* **B492** (2000) 115;
G. Eyal, Y. Nir and G. Perez, *JHEP* **0008** (2000) 028;
A.J. Buras, F. Parodi and A. Stocchi, *JHEP* **0301** (2003) 029.
- [15] Ya.I. Azimov, V.L. Rappoport and V.V. Sarantsev, *Z. Phys.* **A356** (1997) 437;
Y. Grossman and H.R. Quinn, *Phys. Rev.* **D56** (1997) 7259;
J. Charles *et al.*, *Phys. Lett.* **B425** (1998) 375;
B. Kayser and D. London, *Phys. Rev.* **D61** (2000) 116012;
H.R. Quinn *et al.*, *Phys. Rev. Lett.* **85** (2000) 5284.
- [16] A.S. Dighe, I. Dunietz and R. Fleischer, *Phys. Lett.* **B433** (1998) 147;
I. Dunietz, R. Fleischer and U. Nierste, *Phys. Rev.* **D63** (2001) 114015.
- [17] R. Itoh, KEK-PREPRINT-2002-106 [hep-ex/0210025].
- [18] M. Gronau and D. Wyler, *Phys. Lett.* **B265** (1991) 172;
D. Atwood, I. Dunietz and A. Soni, *Phys. Rev. Lett.* **78** (1997) 3257;
R. Fleischer and D. Wyler, *Phys. Rev.* **D62** (2000) 057503.
Y. Grossman, Z. Ligeti and A. Soffer, LBNL-51630 [hep-ph/0210433];
M. Gronau, CERN-TH/2002-331 [hep-ph/0211282].
- [19] J.P. Silva and A. Soffer, *Phys. Rev.* **D61** (2000) 112001;
D. Atwood, I. Dunietz and A. Soni, *Phys. Rev.* **D63** (2001) 036005.
- [20] R. Fleischer, CERN-TH/2003-010 [hep-ph/0301255].
- [21] R. Fleischer, CERN-TH/2003-011 [hep-ph/0301256].
- [22] R. Fleischer, *Phys. Lett.* **B459** (1999) 306.
- [23] A.J. Buras and R. Fleischer, *Phys. Rev.* **D64** (2001) 115010.
- [24] M. Ciuchini, E. Franco, A. Masiero and L. Silvestrini, hep-ph/0212397;
R. Harnik, D.T. Larson, H. Murayama and A. Pierce, hep-ph/0212180.
- [25] R. Fleischer and T. Mannel, *Phys. Lett.* **B511** (2001) 240.
- [26] J.S. Hagelin, S. Kelley and T. Tanaka, *Nucl. Phys.* **B415** (1994) 293;
F. Gabbiani *et al.*, *Nucl. Phys.* **B477** (1996) 321.
- [27] G. Buchalla, A.J. Buras and M.E. Lautenbacher, *Rev. Mod. Phys.* **68** (1996) 1125.
- [28] D. Choudhury *et al.*, *Phys. Lett.* **B342** (1995) 180.
- [29] E. Lunghi, A. Masiero, I. Scimemi and L. Silvestrini, *Nucl. Phys.* **B568** (2000) 120.
- [30] A.J. Buras, A. Romanino and L. Silvestrini, *Nucl. Phys.* **B520** (1998) 3.
- [31] R. Barbieri and A. Strumia, *Nucl. Phys.* **B508** (1997) 3.

- [32] G. Colangelo and G. Isidori, *JHEP* **09** (1998) 009;
A. Masiero and H. Murayama, *Phys. Rev. Lett.* **83** (1999) 907.
- [33] A.J. Buras *et al.*, *Nucl. Phys.* **B566** (2000) 3.
- [34] K.S. Babu and C.F. Kolda, *Phys. Rev. Lett.* **84** (2000) 228;
A.J. Buras *et al.*, *Nucl. Phys.* **B619** (2001) 434;
G. Isidori and A. Retico, *JHEP* **0111** (2001) 001.
- [35] B. Aubert *et al.* (BaBar Collaboration), *Phys. Rev. Lett.* **89** (2002) 281802.
- [36] K. Abe *et al.* (Belle Collaboration), Belle preprint 2003-1 [hep-ex/0301032].
- [37] Particle Data Group (K. Hagiwara *et al.*), *Phys. Rev.* **D66** (2002) 010001.
- [38] M. Gronau and J.L. Rosner, *Phys. Rev.* **D65** (2002) 093012.
- [39] M. Beneke *et al.*, *Nucl. Phys.* **B606** (2001) 245.
- [40] A.I. Sanda and K. Ukai, *Prog. Theor. Phys.* **107** (2002) 421;
Y.-Y. Keum, DPNU-02-30 [hep-ph/0209208]
- [41] M. Gronau and D. London, *Phys. Rev. Lett.* **65** (1990) 3381;
R. Fleischer and T. Mannel, *Phys. Lett.* **B397** (1997) 269;
Y. Grossman and H.R. Quinn, *Phys. Rev.* **D58** (1998) 017504;
J. Charles, *Phys. Rev.* **59** (1999) 054007;
D. London, N. Sinha and R. Sinha, *Phys. Rev.* **D63** (2001) 054015;
M. Gronau, D. London, N. Sinha and R. Sinha, *Phys. Lett.* **B514** (2001) 315;
M. Gronau and J.L. Rosner, *Phys. Rev.* **D66** (2002) 053003.
- [42] K. Anikeev *et al.*, FERMILAB-Pub-01/197 [hep-ph/0201071].
- [43] P. Ball *et al.*, CERN-TH/2000-101 [hep-ph/0003238], in CERN Report on Standard Model physics (and more) at the LHC (CERN, Geneva, 2000) p. 305.
- [44] CLEO Collaboration (A. Bornheim *et al.*), CLEO 03-03 [hep-ex/0302026].
- [45] BaBar Collaboration (B. Aubert *et al.*), hep-ex/0207065; hep-ex/0206053.
- [46] Belle Collaboration (B.C. Casey *et al.*), *Phys. Rev.* **D66** (2002) 092002.
- [47] R. Fleischer and J. Matias, *Phys. Rev.* **D61** (2000) 074004.
- [48] Y. Grossman, B. Kayser and Y. Nir, *Phys. Lett.* **B415** (1997) 90.
- [49] H. Fritzsch and Z.-Z. Xing, *Nucl. Phys.* **B556** (1999) 49.
- [50] M. Neubert and J.L. Rosner, *Phys. Lett.* **B441** (1998) 403; *Phys. Rev. Lett.* **81** (1998) 5076.
- [51] A.J. Buras and R. Fleischer, *Eur. Phys. J.* **C16** (2000) 97; **C11** (1999) 93.

- [52] J.L. Rosner, EFI-02-96 [hep-ph/0207197];
M. Neubert, CLNS-02-1794 [hep-ph/0207327];
R. Fleischer, CERN-TH/2002-293 [hep-ph/0210323].
- [53] W.S. Hou, J.G. Smith and F. Würthwein, NTU-HEP-99-25 [hep-ex/9910014].
- [54] M. Gronau and J.L. Rosner, *Phys. Rev.* **D59** (1999) 113002;
M. Neubert, *JHEP* **9902** (1999) 014;
J. Matias, *Phys. Lett.* **B520** (2001) 131 and hep-ph/0209331.
- [55] E787 Collaboration (S. Adler *et al.*), *Phys. Rev. Lett.* **88** (2002) 041803.
- [56] G. Buchalla and A.J. Buras, *Phys. Lett.* **B333** (1994) 221; *Phys. Rev.* **D54** (1996) 6782.
- [57] G. Buchalla and A.J. Buras, *Nucl. Phys.* **B548** (1999) 309; **B412** (1994) 106.
- [58] S.H. Kettell, L.G. Landsberg and H.H. Nguyen, FERMILAB-FN-0727 [hep-ph/0212321].
- [59] A.J. Buras, TUM-HEP-402-01 [hep-ph/0101336].
- [60] L. Lellouch, CPT-2002-P-4443 [hep-ph/0211359].
- [61] CDF Collaboration (F. Abe *et al.*), *Phys. Rev.* **D57** (1998) 3811.
- [62] BaBar Collaboration (B. Aubert *et al.*), BABAR-CONF-02/028 [hep-ex/0207083].